AGT

Algebraic & Geometric Topology

Volume 25 (2025)

A note on knot Floer homology of satellite knots with (1, 1)-patterns

WEIZHE SHEN

msp

msp

Algebraic & Geometric Topology **25**:6 (2025) 3271–3286
DOI: 10.2140/agt.2025.25.3271
Published: 1 October 2025

A note on knot Floer homology of satellite knots with (1, 1)-patterns

WEIZHE SHEN

We prove that if P is a $(1,1)$-pattern, then the two inequalities $\dim \widehat{\mathrm{HFK}}(P(K)) \geqslant \dim \widehat{\mathrm{HFK}}(P(U))$ and $\dim \widehat{\mathrm{HFK}}(P(K)) \geqslant \dim \widehat{\mathrm{HFK}}(K)$ hold for the unknot $U \subset S^3$ and any companion $K \subset S^3$.

57K18

1 Introduction

Knot Floer homology, introduced independently by Ozsváth and Szabó [18] and J Rasmussen [20], is a powerful invariant of knots in the three-sphere. For example, it captures several geometric properties of knots such as genus (see Ozsváth and Szabó [17]) and fiberedness (see Ghiggini [4] and Ni [15]). The theory has several different variants; here we assume the reader is familiar with the hat version, which takes the form of a bigraded finitely generated vector space over the field $\mathbb{F} := \mathbb{Z}/2\mathbb{Z}$:

$$\widehat{\mathrm{HFK}}(K) = \bigoplus_{m,a\in\mathbb{Z}} \widehat{\mathrm{HFK}}_m(K,a).$$

Here K is a knot in S^3, m is the *Maslov* (or *homological*) grading, and a is the *Alexander* grading.

To three-manifolds with parametrized boundary, Lipshitz, Ozsváth, and Thurston [14] associated bordered Heegaard Floer invariants. Moreover, their pairing theorems are well-adapted to the study of the result of gluing two manifolds with torus boundary. Recall that given a knot P (namely, a pattern) embedded in a standard solid torus $S^1 \times D^2 =: V$ and a knot K (namely, a companion) in S^3, the satellite knot $P(K)$ is obtained from P by gluing V to the complement $X_K := \overline{S^3 - \nu(K)}$ — where $\nu(K)$ is a tubular neighborhood of K — in such a way that the meridian of V is identified with the meridian of K, and the longitude of V is identified with the Seifert longitude of K. Therefore, satellite knots can be studied using bordered Heegaard Floer homology. Some early work in this approach includes that of Hom [10], Levine [13], and Petkova [19]. By definition, a pattern is called (1,1) if it admits a genus-one doubly pointed bordered Heegaard diagram. This note concerns $(1,1)$-patterns and satellite knots with such patterns (which hereinafter may be referred to as $(1,1)$-satellites for short). Moreover, we do not consider patterns that lie in a three-ball in V; that is, we assume that any pattern $P \subset V$ is geometrically essential. We call a pattern *unknotted* if it is isotopic to the core of the solid torus containing it. We do not distinguish unknotted patterns and will denote such a pattern by $\mathfrak{U}$. We reserve U for the unknot in S^3.

For three-manifolds with a single toroidal boundary component, Hanselman, Rasmussen, and Watson [5; 6] interpreted the relevant bordered Heegaard Floer invariants geometrically as decorated immersed curves in the once-punctured torus. Later, a formula for the behavior of these immersed curves under cabling was given by Hanselman and Watson [7]. More recently, Chen [2] studied the computation of knot Floer chain complexes of $(1,1)$-satellites by using immersed curves.

Does a nonzero-degree map give a rank inequality on Heegaard Floer homology? More specifically, Hanselman, Rasmussen, and Watson [6, Question 12] asked, if there is a degree-one map $Y_1 \to Y_2$ between closed connected orientable three-manifolds, is it the case that $\dim \widehat{\mathrm{HF}}(Y_1) \geq \dim \widehat{\mathrm{HF}}(Y_2)$? For integer homology spheres, Karakurt and Lidman [12, Conjecture 9.4] proposed that if there is a nonzero-degree map $Y_1 \to Y_2$ between them, then $\operatorname{rank} \mathrm{HF}_{\mathrm{red}}(Y_1) \geq \operatorname{rank} \mathrm{HF}_{\mathrm{red}}(Y_2)$ and $\operatorname{rank} \widehat{\mathrm{HF}}(Y_1) \geq \operatorname{rank} \widehat{\mathrm{HF}}(Y_2)$. Karakurt and Lidman [12, Theorem 1.9] also studied maps between Seifert homology spheres. It is natural to ask similar questions about knot complements in S^3 and rank inequalities on knot Floer homology. Given a degree-one map $\varphi\colon X_K \to X_U$ that preserves peripheral structure,[1] the induced map $\tilde{\varphi}\colon X_{P(K)} \to X_{P(U)}$ is well-defined and further induces an epimorphism $\tilde{\varphi}_*\colon \pi_1(X_{P(K)}) \to \pi_1(X_{P(U)})$ that also preserves peripheral structure. This is a special case of [11, Question 1.9], in which Juhász and Marengon asked, for knots K_1 and K_2 in S^3 such that there is an epimorphism $\pi_1(X_{K_1}) \to \pi_1(X_{K_2})$ preserving peripheral structure, is it true that $\dim \widehat{\mathrm{HFK}}(K_1) \geq \dim \widehat{\mathrm{HFK}}(K_2)$? We state the version corresponding to the special case $\pi_1(X_{P(K)}) \to \pi_1(X_{P(U)})$ in the following conjecture:

Conjecture 1.1 *Given any pattern P in $S^1 \times D^2$ and any companion K in S^3, there is an inequality $\dim \widehat{\mathrm{HFK}}(P(K)) \geq \dim \widehat{\mathrm{HFK}}(P(U))$, where U denotes the unknot in S^3.*

Another closely related conjecture is the following:

Conjecture 1.2 *Given any pattern P in $S^1 \times D^2$ and any companion K in S^3, there is an inequality $\dim \widehat{\mathrm{HFK}}(P(K)) \geq \dim \widehat{\mathrm{HFK}}(K)$.*

Our purpose here is to prove Conjectures 1.1 and 1.2 when P is a $(1,1)$-pattern, by using (geometrically interpreted) bordered Heegaard Floer invariants.

Theorem 1.3 *Given a $(1,1)$-pattern $P \subset S^1 \times D^2$, the inequality*

$$\dim \widehat{\mathrm{HFK}}(P(K)) \geq \dim \widehat{\mathrm{HFK}}(P(U)) \tag{1}$$

holds for any companion $K \subset S^3$, where U denotes the unknot in S^3.

Theorem 1.4 *Given a $(1,1)$-pattern $P \subset S^1 \times D^2$, the inequality*

$$\dim \widehat{\mathrm{HFK}}(P(K)) \geq \dim \widehat{\mathrm{HFK}}(K) \tag{2}$$

holds for any companion $K \subset S^3$. Moreover, the equality holds if and only if the pattern P is unknotted in $S^1 \times D^2$, or both the companion K and the satellite $P(U)$ are unknotted in S^3.

[1] We refer the reader to Boileau, Boyer, Rolfsen, and Wang [1, Proposition 1] for a proof of the existence of such a map.

Two natural questions (which were originally pointed out by Tye Lidman) to ask are the following:

Question 1.5 *Is it possible to characterize the equality condition for Theorem 1.3?*

Question 1.6 *Does either of the above theorems have a refinement for Maslov gradings?*

Although these two questions are not fully resolved here, we discuss them in detail in Section 4. We will also see that there is no refinement for Alexander gradings.

We conclude this section by briefly explaining two major parts in proving the above theorems. To begin with, the main result of Chen [2] allows us to obtain the dimension of $\widehat{\mathrm{HFK}}(P(K))$ by counting the minimum intersections of the curves $\beta(P)$ and $\alpha(K)$ in its corresponding pairing diagram (which is defined in Section 2):

Theorem 1.7 [2, Theorem 1.2] *Given a* (1,1)*-pattern* $P \subset S^1 \times D^2$ *and a companion* $K \subset S^3$*, let* $\widehat{\mathrm{HF}}(X_K) \subset \partial X_K \setminus \{w'\}$ *be the immersed curves of the knot complement* X_K*, and let* $(\beta, \mu, \lambda, w, z) \subset \partial(S^1 \times D^2)$ *be a five-tuple corresponding to a genus-one doubly pointed bordered Heegaard diagram for* P*. Let* $h\colon \partial X_K \to \partial(S^1 \times D^2)$ *be an orientation-preserving homeomorphism such that*

(i) *h identifies the meridian and Seifert longitude of K with μ and λ, respectively,*

(ii) $h(w') = w$,

(iii) *there is a regular neighborhood $U \subset \partial(S^1 \times D^2)$ of w such that $z \in U$, $U \cap (\lambda \cup \mu) = \varnothing$, and $U \cap h(\widehat{\mathrm{HF}}(X_K)) = \varnothing$.*

Let $\alpha = h(\widehat{\mathrm{HF}}(X_K))$*. Then there is a chain homotopy equivalence*

$$\widehat{\mathrm{CFK}}(\alpha, \beta, w, z) \cong \widehat{\mathrm{CFK}}(S^3, P(K)).$$

Moreover, if α is connected, this chain homotopy equivalence preserves the Maslov grading and Alexander filtration.

Besides Chen's theorem, the proof of Hanselman, Rasmussen, and Watson [6, Theorem 52] is another inspiration for an essential part of our proof — applying a sequence of moves to curves without increasing intersection numbers. Moreover, Theorem 1.4 is close to [6, Theorem 11], which is a special case of [6, Theorem 52].

Acknowledgements

I would like to thank my advisor, Jennifer Hom, for suggesting this problem, and I cannot thank her enough for her continued support, guidance, and patience. I am grateful to Wenzhao Chen and Tye Lidman for constructive comments on an earlier draft and to Steven Sivek for informative email correspondence. I would also like to thank the referee and Matthew Hedden for their insightful suggestions.

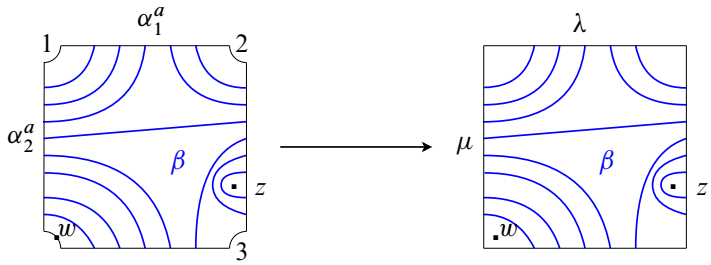

Figure 1: The data contained in a genus-one doubly pointed bordered Heegaard diagram (on the left) of the Mazur pattern can be equivalently understood as a five-tuple (on the right). This convention comes from [2, Sections 1 and 5].

2 Preliminaries

In this section, we primarily recapitulate some conventions and results in [2; 3] and then set up several notations, in preparation for proving Theorems 1.3 and 1.4 in Section 3.

We begin with a more thorough discussion about Theorem 1.7. The five-tuple in Theorem 1.7 is obtained from a genus-one doubly pointed bordered Heegaard diagram, $(\overline{\Sigma}, \{\alpha_1^a, \alpha_2^a\}, \beta, w, z)$, of P. This is done by viewing β, w, and z as embedded in $\partial(S^1 \times D^2)$ and identifying the pair of arcs $\{\alpha_1^a, \alpha_2^a\}$ with the longitude–meridian pair of $\partial(S^1 \times D^2)$. See Figure 1 for an example of the Mazur pattern.

In practice, Theorem 1.7 shows that, after identifying the torus $\partial(S^1 \times D^2)$ with the quotient space $[0,1]\times[0,1]/\sim$ in the standard way and dividing the unit square evenly into four quadrants, we can fit $\alpha = \widehat{\mathrm{HF}}(X_K)$ into the first quadrant $\left[\frac{1}{2}, 1\right]\times\left[\frac{1}{2}, 1\right]$, fit (β, w, z) into the third quadrant $\left[0, \frac{1}{2}\right]\times\left[0, \frac{1}{2}\right]$, and extend them both horizontally and vertically to obtain a diagram that yields a chain complex isomorphic to $\widehat{\mathrm{CFK}}(P(K))$. We call such a diagram a *pairing diagram* for $P(K)$, and we denote by $\alpha(K)$ and $\beta(P)$ the curves obtained from α and β by extension, respectively. Figure 2 displays four examples, in which M denotes the Mazur pattern, $T_{p,q}$ denotes the (p,q)-torus knot, and $K_{p,q}$ denotes the (p,q)-cable of a knot K.

The proof of Theorem 1.3 needs some caution, as we will be moving α-curves, which are immersed in general. The following lemma, which is widely known as the *Whitney–Graustein theorem*, allows us to get rid of self-intersections of immersed curves (after certain modifications, which will be explained in Section 3).

Lemma 2.1 ([21, Theorem 1]; see also [3, Theorem 1]) *Regular homotopy classes of regular closed curves $\bar{\gamma}: S^1 \to \mathbb{R}^2$ are in one-to-one correspondence with the integers, the correspondence being given by*

$$[\bar{\gamma}] \mapsto \mathrm{rot}(\bar{\gamma}),$$

where $\mathrm{rot}(\bar{\gamma})$ *is the degree*[2] *of the map* $S^1 \to \mathbb{R}^2\backslash\{\mathbf{0}\}$, $s \mapsto \bar{\gamma}'(s)$.

[2] By [3], the integer $\mathrm{rot}(\bar{\gamma})$ is called the *rotation number* of $\bar{\gamma}$, and it is a signed count of the number of complete turns of the velocity vector $\bar{\gamma}'$ as we traverse $\bar{\gamma}$ in a prefixed orientation.

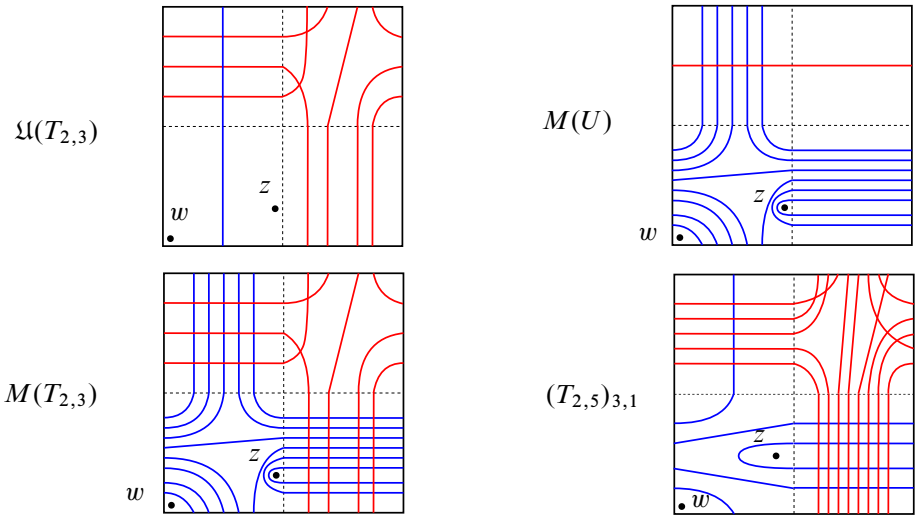

Figure 2: Examples of paring diagrams. The curves $\beta(P)$ and $\alpha(K)$ are drawn in blue and red, respectively.

The last thing we recall here is how to obtain α-curves from immersed curves in a (punctured) infinite cylinder, and vice versa. Given immersed curves in $\left(\mathbb{R}/\left(\frac{1}{2}+\mathbb{Z}\right)\right)\times\mathbb{R}$, we place a grid system consisting of two vertical columns of unit squares, with the middle vertices identified with the punctured points of the cylinder. Then we follow the curve and replicate its segment in a square every time we meet an edge of a grid square. In this way, we build its corresponding α-curves. Likewise, if we start with a torus with α-curves, we can trace the curves and recover its immersed curves in an infinite cylinder, as illustrated in Figure 3.

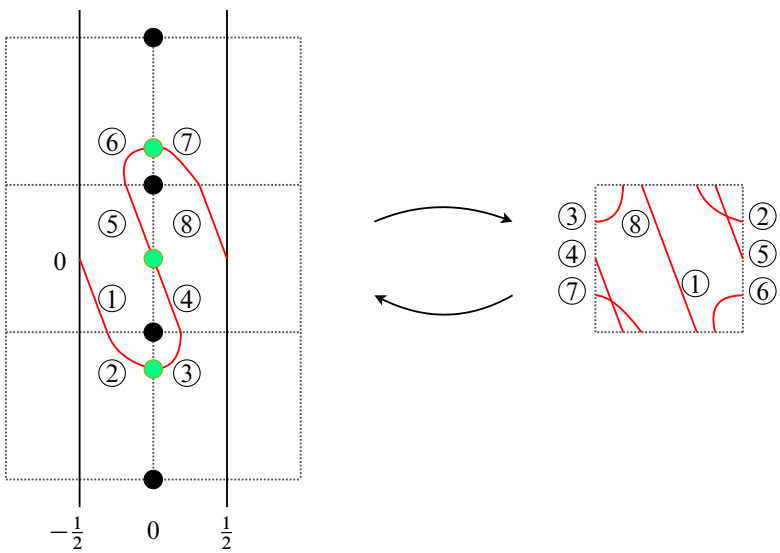

Figure 3: The immersed curve for $-T_{2,3}$ in an infinite cylinder (left) and the α-curves for $-T_{2,3}$ in a torus (right), where the circled numbers can be used to follow the construction.

3 Proof of theorems

Proof of Theorem 1.3 Given a $(1,1)$-pattern $P \subset S^1 \times D^2$ and a companion knot $K \subset S^3$, let $(T^2, \alpha(K), \beta(P), w, z)$ be a pairing diagram for $P(K)$, where $T^2 \cong S^1 \times S^1$. Lift the diagram to $\mathbb{R}^2$ by the covering map $\pi := p \times p : \mathbb{R}^2 \to T^2$, where $p : \mathbb{R} \to S^1$ is given by $x \mapsto (\cos(2\pi x), \sin(2\pi x))$. Let β_0 be a lift of $\pi^{-1}(\beta(P))$. By the construction of $\beta(P)$, the lift β_0 is connected. (See Figure 4 for an example of the Mazur pattern, where the lifts of extended α-curves are omitted.) Let α_0 be a lift of $\alpha(K)$. Notice that α_0 may not be connected, for the immersed curves α may consist of multiple components. (See Figure 5 for an example of the right-handed trefoil, where the lifts of extended β-curves are omitted.)

By [7, page 3], any immersed multicurve in an infinite cylinder has a unique component wrapping around the cylinder. Then the construction at the end of Section 2 implies that there is at least one horizontal line segment in the second quadrant of $(T^2, \alpha(K), \beta(P), w, z)$. Thus, the lift α_0 contains horizontal line segments.

Ignore any closed component that α_0 may contain. Then α_0 becomes a connected piece going to the left- and right-infinity on $\mathbb{R}^2$. (Note that we may lose some data by doing so; nevertheless, we shall see by the end of the proof that (1) still holds.) Without loss of generality, give α_0 an overall rightward orientation. Then there exist rightward-oriented horizontal line segments in α_0; indeed, otherwise, α_0 would not extend to the right infinity. Tracing α_0 from left to right, denote by μ_1 the first such segment

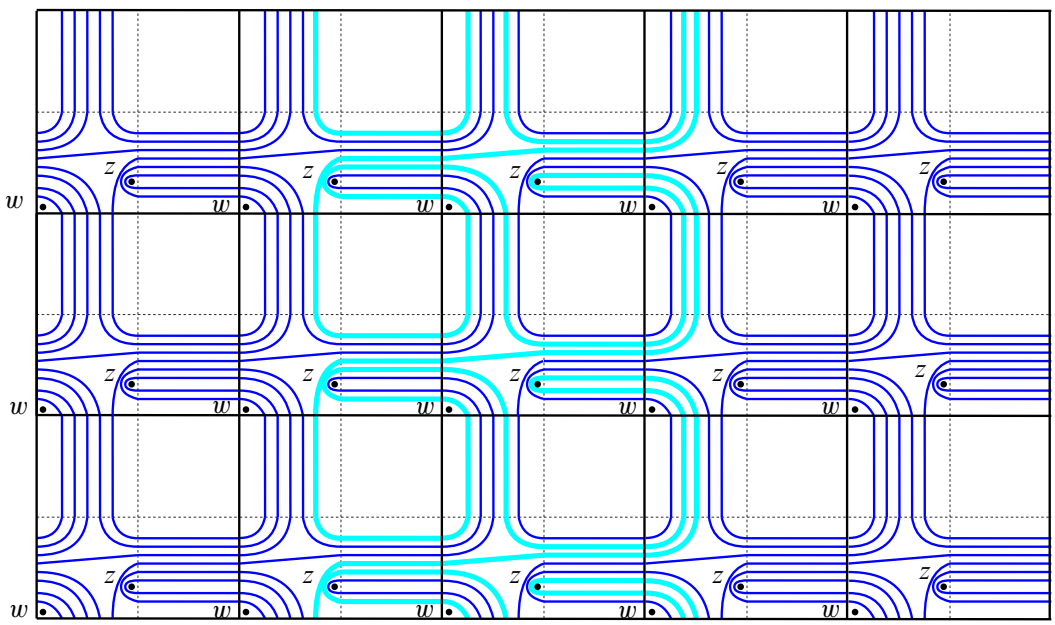

Figure 4: A choice of β_0 (highlighted in cyan) that corresponds to the Mazur pattern. (With a slight abuse of notation, we use the same symbols, w and z, for the lifts of the two basepoints, respectively.)

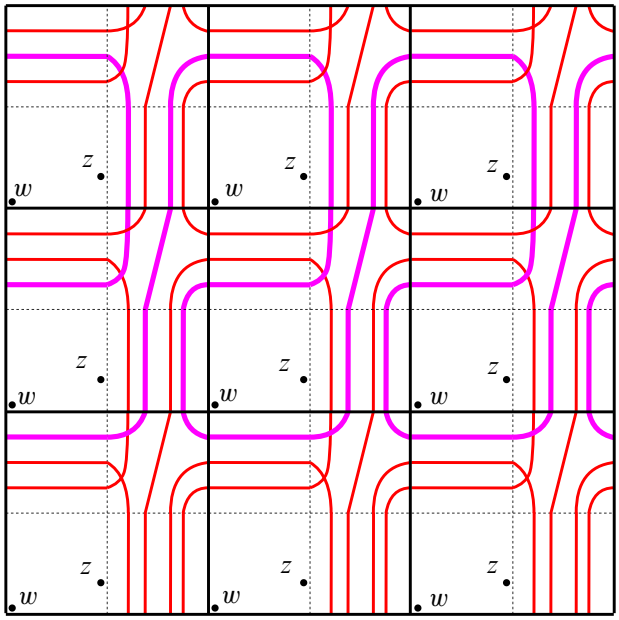

Figure 5: A choice of α_0 (highlighted in magenta) that corresponds to $T_{2,3}$.

that intersects β_0. Without loss of generality, suppose that $\mu_1 \subset \left[0, \frac{1}{2}\right] \times \left[\frac{1}{2}, 1\right]$. Consider the set $\mathcal{M} := \pi^{-1}(\pi(\mu_1)) \cap ([1,\infty) \times [0,1])$, which consists of all lifts of $\pi(\mu_1)$ that lie in $[1,\infty) \times [0,1]$. For each element in $\mathcal{M}$, denote it by μ_j if it lies in $[j-1, j] \times [0,1]$. Let $k := \max\{j \mid \mu_j \cap \beta_0 \neq \varnothing\}$, and let α_0^* denote the connected portion of α_0 between μ_1 and μ_{k+1}, with μ_1 included and μ_{k+1} excluded. (See Figure 6 for an illustration, where the segments μ_j are highlighted in green.)

Notice that α_0 is periodic, exhibiting horizontal translational symmetry, so α_0^* is periodic as well. Moreover, α_0^* consists of k periods, with the j^{th} period of α_0^* starting from μ_j and terminating at the left endpoint of μ_{j+1}, for $j = 1, 2, \ldots, k$, if we traverse α_0^* from left to right.

As we mentioned in Section 2, the curve α_0^* may contain self-intersections; we claim that all of them can be resolved by regular homotopies (which are allowed to cross any lift of basepoints). Indeed, we can complete α_0^* into an immersed closed curve by attaching the top endpoint of a left semicircle of radius R to the left endpoint of μ_1, attaching the top endpoint of a right semicircle of radius R to the left endpoint of μ_{k+1}, and then connecting the two bottom endpoints of these two semicircles by a line segment, where R is sufficiently large so that the newly added three segments do not intersect α_0^*. By the 180° symmetry of immersed curves for knot complements (up to regular homotopy), the turning number induced from each self-intersection will be canceled by that of its symmetric counterpart, so overall, the rotation number of the closed curve we just created is ± 1, depending on its orientation. By Lemma 2.1, this rotation number is preserved under regular homotopies, so this closed curve is in the class of circles. Therefore, we can resolve all possible self-intersections of α_0^*.

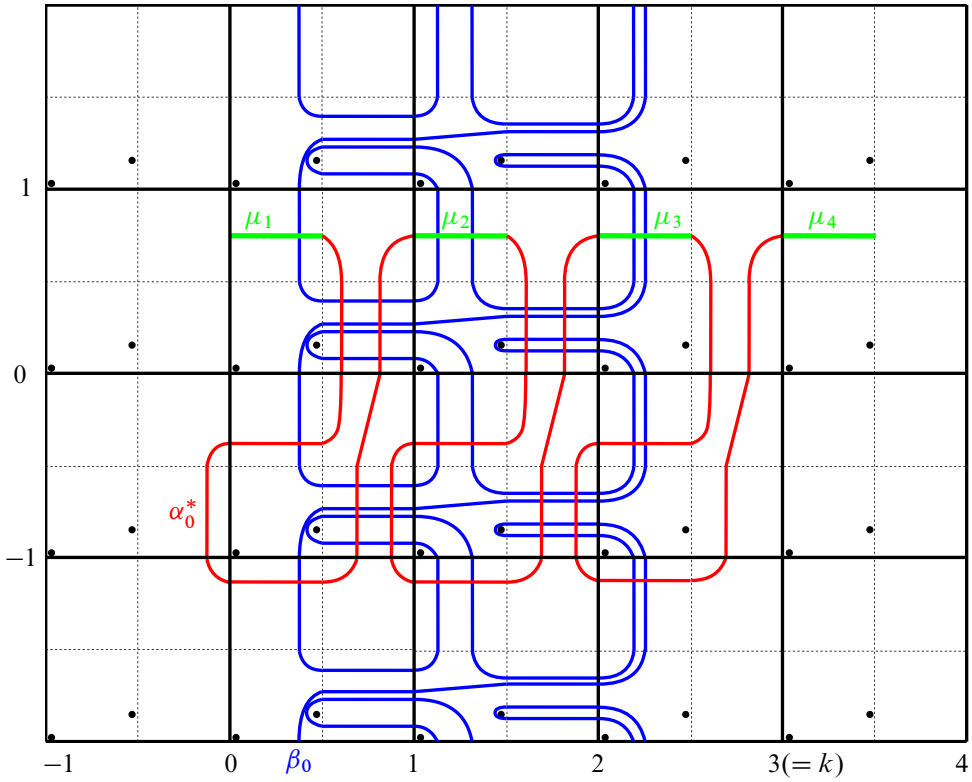

Figure 6: An example of $M(T_{2,3})$.

For each $j \in \{1, 2, \dots, k\}$, consider (the closure of) the complement of μ_j in the j^{th} period of α_0^*. Allowing passing lifts of basepoints, regularly homotope this complement with its two endpoints fixed until the curve is within $\left[j-\frac{1}{2}, j\right] \times \left[\frac{1}{2}, 1\right]$. By the claim above, we may assume all self-intersections have been resolved, so we can further regularly homotope α_0^* until it becomes a horizontal line segment in $[0,k] \times \left[\frac{1}{2}, 1\right]$. We call the resulting curve $\alpha_0^{*'}$.

Since $\alpha(U)$ is a horizontal line segment, the α_0-curve that corresponds to the unknot U, denoted by $\alpha_0(U)$, is a horizontal line in $\mathbb{R} \times \left[\frac{1}{2}, 1\right]$. Moreover, $\alpha_0(U)$ first intersects β_0 in the square $[0,1] \times [0,1]$ and lastly in $[k-1, k] \times [0,1]$, by the definitions of μ_1 and k. Therefore, to get the dimension of $\widehat{\mathrm{HFK}}(P(U))$, it suffices to consider β_0 and the portion of $\alpha_0(U)$ lying in $[0,k] \times \left[\frac{1}{2}, 1\right]$. We denote this portion by $\alpha_0^*(U)$, which is exactly the α_0^*-curve that corresponds to U, and moreover, it can be identified with $\alpha_0^{*'}$.

Consider the set $\alpha_0^{*'} \cap \beta_0$ of intersection points. For each pair $x, y \in \alpha_0^{*'} \cap \beta_0$ that form the two vertices of an empty bigon (ie a bigon that has no basepoint inside) between $\alpha_0^{*'}$ and β_0, we denote the bigon by $B_{x,y}$ and take a sufficiently small open neighborhood $U_{x,y} \supset B_{x,y}$ such that

(i) no basepoint is inside, and

(ii) after we regularly homotope β_0 inside $U_{x,y}$ to eliminate the empty bigon, no new intersection point is generated.

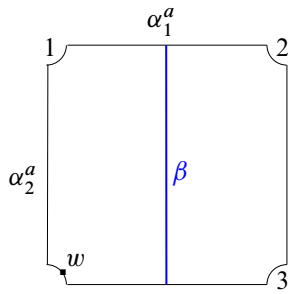

Figure 7: The genus-one bordered Heegaard diagram of $S^1 \times D^2$, up to isotopy.

Condition (ii) can be achieved since we are considering finitely many segments in $\mathbb{R}^2$. If multiple bigons are nested, then we start with the innermost one, and in this order, (ii) can still be achieved. By the definition of $U_{x,y}$, each move of β_0 does not cross basepoints. Therefore, after all such empty bigons are eliminated, we obtain a minimum intersection diagram between $\alpha_0^{*'}$ and β_0, and the final intersection number equals $\dim \widehat{\mathrm{HFK}}(P(U))$.

Observe that the sequence of moves described above eliminates all empty bigons generated by α_0^* and β_0 and does not increase the number of intersections with β_0, the number of intersections between α_0^* and β_0 is at most the number of intersections between the original α_0 and β_0, and the minimum intersection number (obtained by eliminating empty bigons via regular homotopies without passing basepoints) between the original α_0 and β_0 gives $\dim \widehat{\mathrm{HFK}}(P(K))$. These observations, together with the result in the above paragraph, imply that $\dim \widehat{\mathrm{HFK}}(P(K)) \geq \dim \widehat{\mathrm{HFK}}(P(U))$. □

Remark 3.1 In the proof above, we applied regular homotopies in the covering space $\mathbb{R}^2$ of T^2. Recall that the covering map π is defined as $p \times p$, where $p\colon \mathbb{R} \to S^1$ is given by $x \mapsto (\cos(2\pi x), \sin(2\pi x))$. Composing those regular homotopies with π, we shall get regular homotopies in the base space T^2.

Proof of Theorem 1.4 Here we continue with the curves α_0 and β_0 that have been set up in the first paragraph of the proof of Theorem 1.3.

Recall that the five-tuple $(\beta, \mu, \lambda, w, z) \subset \partial(S^1 \times D^2)$ is constructed from a genus-one doubly pointed bordered Heegaard diagram, say $(\overline{\Sigma}, \{\alpha_1^a, \alpha_2^a\}, \beta, w, z)$, for $(S^1 \times D^2, P)$. Forgetting the z-basepoint, we obtain a genus-one bordered Heegaard diagram for the solid torus $S^1 \times D^2$ with the standard parametrization of $\partial(S^1 \times D^2)$. Therefore, up to isotopy (not passing the w-basepoint), the diagram $(\overline{\Sigma}, \{\alpha_1^a, \alpha_2^a\}, \beta, w)$ is in the form shown in Figure 7.

It then follows from the construction of the curve β_0 that, if we forget the basepoint z, we can isotope β_0 without passing any lift of the basepoint w until it becomes a vertical straight line; we denote the line by β_0'. See Figure 8 for an illustration.

Since the β-curve associated with the unknotted pattern $\mathfrak{U}$ is a vertical line segment, the corresponding β_0-curve, denoted by $\beta_0(\mathfrak{U})$, is a vertical line in $\mathbb{R}^2$, which can be identified with β_0'. The number

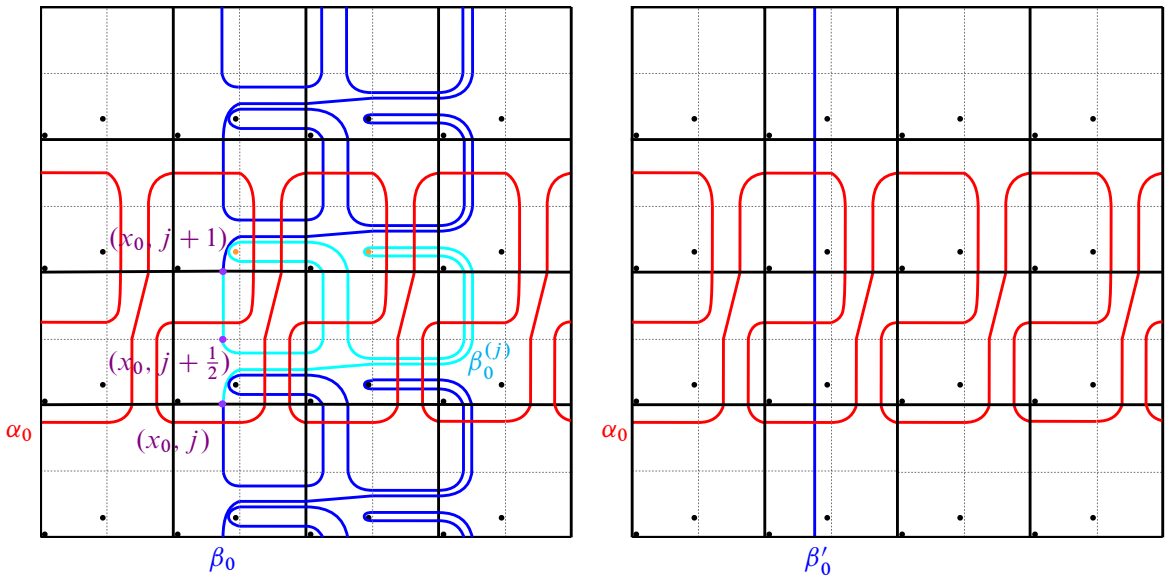

Figure 8: The α_0-, β_0-, and β_0'-curves for $M(T_{2,3})$, in which a β_0-period is highlighted in cyan for some $j \in \mathbb{Z}$.

of intersections between $\beta_0(\mathfrak{U})$ and α_0 gives $\dim \widehat{\mathrm{HFK}}(\mathfrak{U}(K))$; therefore, the number of intersections between β_0' and α_0 is precisely $\dim \widehat{\mathrm{HFK}}(K)$.

Now we compare the pair of curves (α_0, β_0') with the original (α_0, β_0). Observe that the isotopies described above eliminate all empty bigons generated by β_0 and α_0 and do not increase the number of intersections with α_0, and the minimum intersection number (obtained by eliminating empty bigons via isotopies without passing basepoints) between β_0 and α_0 gives $\dim \widehat{\mathrm{HFK}}(P(K))$. These observations, together with the result in the above paragraph, imply that $\dim \widehat{\mathrm{HFK}}(P(K)) \geqslant \dim \widehat{\mathrm{HFK}}(K)$.

In the following, we justify the equality conditions. One direction is clear: If the pattern P is unknotted (ie $P = \mathfrak{U}$), then $\dim \widehat{\mathrm{HFK}}(P(K)) = \dim \widehat{\mathrm{HFK}}(\mathfrak{U}(K)) = \dim \widehat{\mathrm{HFK}}(K)$ for any companion $K \subset S^3$. If both the companion K and the satellite $P(U)$ are unknotted in S^3 (ie $K = U = P(U)$), then $\dim \widehat{\mathrm{HFK}}(P(K)) = \dim \widehat{\mathrm{HFK}}(P(U)) = \dim \widehat{\mathrm{HFK}}(U) = \dim \widehat{\mathrm{HFK}}(K)$.

Next we prove the opposite direction. Assuming that $P \neq \mathfrak{U}$, and that $K \neq U$ or $P(U) \neq U$, we show that we actually have a strict inequality in Theorem 1.4:

$$\dim \widehat{\mathrm{HFK}}(P(K)) > \dim \widehat{\mathrm{HFK}}(K). \tag{3}$$

If $K = U$, then by the assumption we just made $P(U) \neq U$; since knot Floer homology detects the unknot [17, Theorem 1.2], it follows that $\dim \widehat{\mathrm{HFK}}(P(U)) > \dim \widehat{\mathrm{HFK}}(U)$. We may now assume that $K \neq U$ and $P \neq \mathfrak{U}$. Then in terms of the α- and β-curves in the universal cover $\mathbb{R}^2$, α_0 is not a horizontal line and β_0 is not a vertical line. In particular, $y_{\alpha_0}^{\mathrm{top}} - y_{\alpha_0}^{\mathrm{bottom}} > 0$, where $y_{\alpha_0}^{\mathrm{top}}$ and $y_{\alpha_0}^{\mathrm{bottom}}$ are defined as $y_{\alpha_0}^{\mathrm{top}} = \max\{y \in \mathbb{R} \mid (x, y) \in \alpha_0\}$ and $y_{\alpha_0}^{\mathrm{bottom}} = \min\{y \in \mathbb{R} \mid (x, y) \in \alpha_0\}$, respectively, assuming that

a Cartesian coordinate system has been fixed for $\mathbb{R}^2$ beforehand. As for the β_0-curve, we first need to discuss more of its properties in the following paragraph.

We use the notation $\beta_0+(x,y)$, where $x, y\in\mathbb{R}$, to denote the translation of β_0 that is obtained from first sliding it $|x|$ units to the right if $x\geqslant 0$ and to the left if $x<0$, and then sliding it $|y|$ units upward if $y\geqslant 0$ and downward if $y<0$. The fact that the $\beta(P)$-curve is embedded implies that $\beta_0=\beta_0+(0,1)$ and $\beta_0\cap[\beta_0+(\pm 1,0)]=\varnothing$. In words, it means that the β_0-curve is invariant under vertical translations of integral units, and if we consider all the lifts of $\beta(P)$ to $\mathbb{R}^2$, any two of them (in particular, adjacent pairs) are disjoint. Give β_0 an overall downward orientation. Recall that we can isotope β_0, allowing it to pass through the lifts of the z-basepoint but not those of the w-basepoint, to obtain the vertical line β_0'. We may assume that during that process, a vertical line segment $\{x_0\}\times\left[j+\frac{1}{2}, j+1\right]$, where $x_0\in\left(i, i+\frac{1}{2}\right)$ for some $i\in\mathbb{Z}$, is fixed for each $j\in\mathbb{Z}$, and as a result, the vertical line β_0' is $\{x_0\}\times\mathbb{R}$. For each $j\in\mathbb{Z}$, we call the connected part of β_0 that connects the two points $(x_0, j+1)$ and (x_0, j) the j^{th} *period* of β_0 and denote it by $\beta_0^{(j)}$. By our assumption, the vertical line segment $\{x_0\}\times\left[j+\frac{1}{2}, j+1\right]$ is part of $\beta_0^{(j)}$, for each $j\in\mathbb{Z}$. Notice also that these β_0-periods satisfy[3] that $\beta_0^{(j+1)}=\beta_0^{(j)}+(0,1)$, for each $j\in\mathbb{Z}$. Figure 8, left, gives an illustration, in which one β_0-period is highlighted in cyan for some $j\in\mathbb{Z}$, and the points (x_0, j), $\left(x_0, j+\frac{1}{2}\right)$, and $(x_0, j+1)$ are in violet.

We will complete the proof by dividing the possible β_0-curves into three cases and then proving the result in each case, but before introducing them, we need to justify the following claim: For each $j\in\mathbb{Z}$, denoting the infinite horizontal region $\mathbb{R}\times[j, j+1]$ by $\mathcal{H}_j$, if $\beta_0^{(j)}\not\subset\mathcal{H}_j$, then either $\beta_0^{(j)}\cap\operatorname{int}(\mathcal{H}_{j+1})=\varnothing$ or $\beta_0^{(j)}\cap\operatorname{int}(\mathcal{H}_{j-1})=\varnothing$, up to isotopy respecting all basepoints. (Roughly speaking, if a β_0-period $\beta_0^{(j)}$ is not contained in the horizontal region $\mathcal{H}_j$, then it either goes up or down, but not in both directions.) We prove the claim by showing that, if $\beta_0^{(j)}\not\subset\mathcal{H}_j$ and $\beta_0^{(j)}\cap\operatorname{int}(\mathcal{H}_{j+1})\neq\varnothing$, then $\beta_0^{(j)}\cap\operatorname{int}(\mathcal{H}_{j-1})=\varnothing$; the other case is similar. Indeed, if $\beta_0^{(j)}\cap\operatorname{int}(\mathcal{H}_{j-1})\neq\varnothing$, then since β_0 can be isotoped to β_0' without passing through w points, there must be some z point (denoted by z_{j-p}) in some $\mathcal{H}_{j-p}$, where $p\in\mathbb{Z}$ and $p\geqslant 1$, such that $\beta_0^{(j)}$ winds around z_{j-p} (or in other words, the point z_{j-p} blocks $\beta_0^{(j)}$ from isotopies respecting all basepoints). For example, the two orange z points in Figure 8, left, block $\beta_0^{(j)}$ in $\mathcal{H}_{j+1}$. Likewise, since $\beta_0^{(j)}\cap\mathcal{H}_{j+1}\neq\varnothing$, there is some z point (denoted by z_{j+q}) in some $\mathcal{H}_{j+q}$, where $q\in\mathbb{Z}$ and $q\geqslant 1$, such that $\beta_0^{(j)}$ winds around z_{j+q}. Consider the $(j+q+p)^{\text{th}}$ β_0-period. We can deduce from the translational properties of β_0 (which have been discussed in the above paragraph) that some horizontal translation of $\beta_0^{(j+q+p)}$ by an integral unit (which might be 0) winds around the point z_{j+q} as well as $\beta_0^{(j)}$. This, however, results in intersections between that curve and $\beta_0^{(j)}$, contradicting the properties that the lifts of $\beta(P)$ are embedded in $\mathbb{R}^2$ and any two of them are disjoint.

Thanks to the claim above, we can divide the β_0-curves into three cases: $\beta_0^{(j)}\subset\mathcal{H}_j$, $\beta_0^{(j)}\cap\operatorname{int}(\mathcal{H}_{j+1})\neq\varnothing$, and $\beta_0^{(j)}\cap\operatorname{int}(\mathcal{H}_{j-1})\neq\varnothing$, for any $j\in\mathbb{Z}$. We show in the following that in each case the strict inequality (3) holds:

[3] Here we extend the application of the translation notation that was originally defined for β_0.

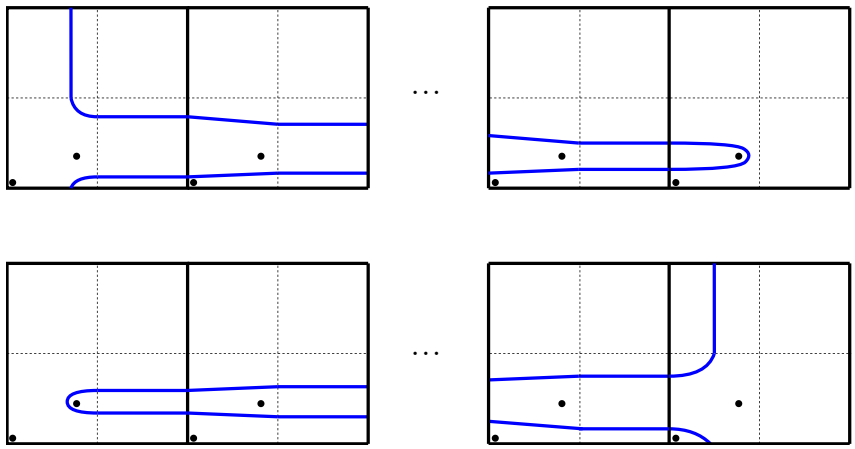

Figure 9: The two cases of a β_0-period when it is contained in a single H_j region.

(I) When $\beta_0^{(j)} \subset \mathcal{H}_j$, each period $\beta_0^{(j)}$ is as depicted in one of the two diagrams in Figure 9, up to isotopy respecting all basepoints. Indeed, if $\beta_0^{(j)}$ appears on both sides of $\beta_0' = \{x_0\} \times \mathbb{R}$, then there exist two integers $n_1, n_2 \in \mathbb{Z}$ with $n_1 + 1 < x_0 < n_2$ such that $\beta_0^{(j)}$ winds around the left side of the z-basepoint in the square $[n_1, n_1 + 1] \times [j, j + 1]$ and winds around the right side of the z-basepoint in the square $[n_2, n_2 + 1] \times [j, j + 1]$. Consider the translation $\beta_0^{(j)} + (n_1 - n_2, 0)$: it winds around the right side of the z-basepoint in the square $[n_1, n_1 + 1] \times [j, j + 1]$, and therefore it intersects with $\beta_0^{(j)}$, which is a contradiction. Comparing Figure 9 with [10, Figure 6], it is not hard to see that the patterns in this case are precisely the $(p, 1)$-cabling patterns, where $p \in \mathbb{Z}$ and $|p| \geqslant 2$. By the formula for the behavior of immersed curves under cabling from [7], if we denote the lift of $\alpha(K)$ to the punctured infinite cylinder $\big(\mathbb{R}/\big(\frac{1}{2} + \mathbb{Z}\big)\big) \times \mathbb{R}$ by $\hat{\alpha}(K)$, then p copies of $\hat{\alpha}(K)$ will be introduced and eventually aligned along the line of punctures. Thus, the number of intersections between the immersed multicurve and the line connecting the punctures strictly increases, which gives us the strict inequality as desired.

(II) If $\beta_0^{(j)} \cap \operatorname{int}(\mathcal{H}_{j+1}) \neq \varnothing$, then $\beta_0^{(j)} \cap \operatorname{int}(\mathcal{H}_{j-1}) = \varnothing$. Let k be the ceiling of $y_{\alpha_0}^{\text{bottom}}$, ie $k \in \mathbb{Z}$ and $y_{\alpha_0}^{\text{bottom}} < k < y_{\alpha_0}^{\text{bottom}} + 1$. The isotopy that takes β_0 to β_0' can be considered as the composition of isotopies, each of which takes one β_0-period into a vertical line segment lying in β_0'. Now in this case, we only partially isotope β_0: we do such isotopies for all the $\beta_0^{(j)}$ where $j \geqslant k$ but leave the remaining β_0-periods as they are. See Figure 10 for an illustration. Note that, by construction, the ray $\beta_0' \cap \big(\{x_0\} \times \big[k - \frac{1}{2}, \infty\big)\big)$ is still part of the β_0-curve after isotopies, and the intersection number between it and α_0 gives us $\dim \widehat{\mathrm{HFK}}(K)$. Now further isotope $\big(\bigcup_{j \leqslant k-1} \beta_0^{(j)}\big) - \{x_0\} \times \big[k - \frac{1}{2}, k\big]$ to eliminate all empty bigons. Since $\beta_0^{(k-1)} \cap \operatorname{int}(\mathcal{H}_k) \neq \varnothing$, it is blocked by at least one z-point above $\mathcal{H}_{k-1}$. For β_0 to reach such a z-point, it is impossible for it to avoid entering the second and fourth quadrants of all unit squares with integral-coordinates vertices. Thus, there must be additional intersections between β_0 and α_0, so the intersection number must exceed $\dim \widehat{\mathrm{HFK}}(K)$. Hence, the inequality (3) holds.

(III) If $\beta_0^{(j)} \cap \operatorname{int}(\mathcal{H}_{j-1}) \neq \varnothing$, then $\beta_0^{(j)} \cap \operatorname{int}(\mathcal{H}_{j+1}) = \varnothing$. The proof of this case is similar to (II). □

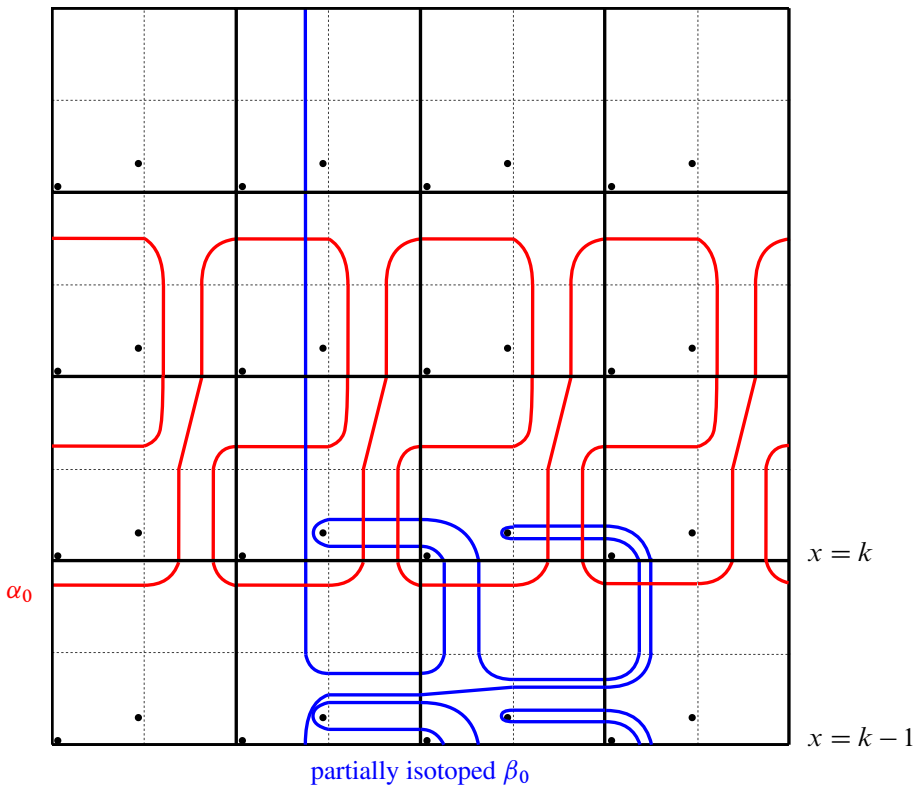

Figure 10: An illustration of how the β_0 curve is partially isotoped as needed in case (II) of the proof of the strict inequality (3). Here k is the ceiling of $y_{\alpha_0}^{\text{bottom}}$.

4 Further remarks

In this section, we make several remarks, further discussing the two inequalities we have proved. In particular, we give more details about the two questions, which were suggested by Jennifer Hom and Lidman, from Section 1.

We begin with an easy observation. A major property of knot Floer homology is that it categorifies the Alexander polynomial $\Delta_K(t)$ of knots $K \subset S^3$ [18]:

$$\Delta_K(t) = \sum_{a\in\mathbb{Z}} \Big[\sum_{m\in\mathbb{Z}} (-1)^m \dim \widehat{\mathrm{HFK}}_m(K,a) \Big] t^a.$$

Also, there is a symmetry [18, Proposition 3.10]:

$$\widehat{\mathrm{HFK}}_m(K,a) \cong \widehat{\mathrm{HFK}}_{m-2a}(K,-a).$$

Since one of the characterizing conditions for Alexander polynomials is that

$$\Delta_K(1) = 1,$$

it follows that the parity of $\dim \widehat{\mathrm{HFK}}(K)$ is odd.

Remark 4.1 Ozsváth and Szabó [17] proved that if $\dim \widehat{\mathrm{HFK}}(K) = 1$ then K is the unknot. Hedden and Watson [9, Corollary 8] showed that if $\dim \widehat{\mathrm{HFK}}(K) = 3$ then K is a (left- or right-handed) trefoil; see also [4, Corollary 1.5]. From these two knot-detecting results, the example depicted in Figure 11 (which shows that there exists a $(1,1)$-satellite K with $\dim \widehat{\mathrm{HFK}}(K) = 5$), and the above parity result, we deduce that if $\dim \widehat{\mathrm{HFK}}(K) < 5$ then K is not a $(1,1)$-satellite.

Next, we discuss some special cases when we have a strict inequality:

Remark 4.2 In the proof of Theorem 1.3, we mentioned that any immersed multicurve in an infinite cylinder has a unique component wrapping around the cylinder. When the set of immersed curves corresponds to a knot complement, this component is an invariant of the knot, and furthermore, an invariant of the concordance class of the knot [7, Proposition 2]. It follows that all slice knots have a trivial such component as the unknot does; in terms of the notation we used in the proof above, with all closed components removed, α_0 is a straight horizontal line. Moreover, for nontrivial slice knots, there are some additional closed components. Therefore, for a nontrivial slice companion knot K, inequality (2) in Theorem 1.4 is strict:

$$\dim \widehat{\mathrm{HFK}}(P(K)) > \dim \widehat{\mathrm{HFK}}(K).$$

In addition to that case, Petkova [19, Lemma 7] showed that the complex $\mathrm{CFK}^-(K)$ for Floer homologically thin knots K splits into exactly one staircase summand and possibly multiple square summands. Geometrically, a square summand is represented by a closed component in α_0, so for Floer homologically thin knots K containing a square summand in $\mathrm{CFK}^-(K)$, the above strict inequality holds as well.

Our last remark is related to gradings:

Remark 4.3 In the proof of Theorem 1.4, we managed to isotope the curve β_0 in a desired way, passing only the z-lifts. Then by Theorem 1.7, if α is connected, and if we only consider Maslov gradings, what we have proved is also true. That is, if α is connected, the inequality

$$\sum_{a\in\mathbb{Z}} \dim \widehat{\mathrm{HFK}}_m(P(K), a) \geqslant \sum_{a\in\mathbb{Z}} \dim \widehat{\mathrm{HFK}}_m(K, a)$$

holds for any Maslov grading $m \in \mathbb{Z}$.

On the other hand, the regular homotopies in the proof of Theorem 1.3 cannot achieve that property in general; for example, Figure 6 shows that we cannot tighten the curve α_0 corresponding to $T_{2,3}$ to a horizontal line without passing any w-lift.

If we just consider Alexander gradings, we will not arrive at rank inequalities that work for all $(1,1)$-satellites. Indeed, consider the example of $(T_{2,3})_{2,3}$, the $(2,3)$-cable of the right-handed trefoil. Since $T_{2,3}$ is alternating, its knot Floer homology is determined by the Alexander polynomial and the knot signature [16], and it is depicted in Figure 11, left. By Hedden's work [8], the knot Floer homology

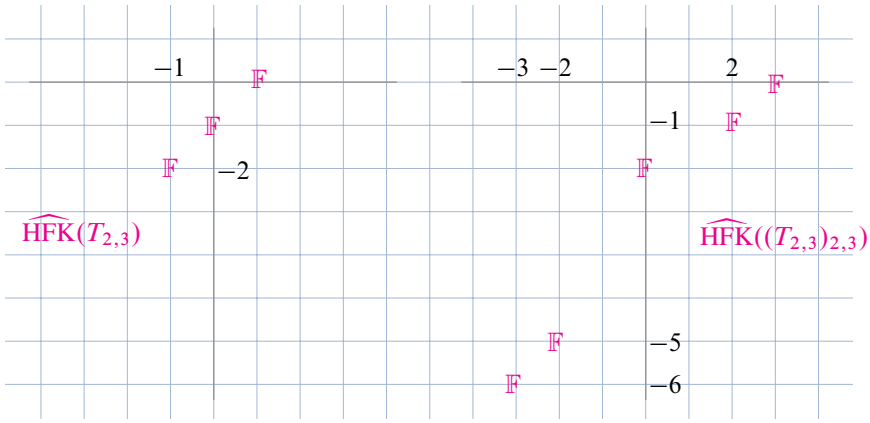

Figure 11: Knot Floer homologies of $T_{2,3}$ and $(T_{2,3})_{2,3}$, plotted on an (a,m)-coordinate system (where the horizontal axis is for a).

of $(T_{2,3})_{2,3}$ can also be determined from its symmetrized Alexander polynomial, and it is depicted in Figure 11, right. This example was originally constructed by Hom; see also [11, Example 1.8]. Now we can make the following observations:

a	$\sum_{m\in\mathbb{Z}} \dim \widehat{\mathrm{HFK}}_m(T_{2,3},a)$	$\sum_{m\in\mathbb{Z}} \dim \widehat{\mathrm{HFK}}_m((T_{2,3})_{2,3},a)$	observations
-2	0	1	$0<1$
-1	1	0	$1>0$
0	1	1	$1=1$

The last column in the above table shows that Theorems 1.3 and 1.4 do not have refinements for Alexander gradings.

References

[1] **M Boileau**, **S Boyer**, **D Rolfsen**, **S C Wang**, *One-domination of knots*, Illinois J. Math. 60 (2016) 117–139 MR Zbl

[2] **W Chen**, *Knot Floer homology of satellite knots with* $(1,1)$ *patterns*, Selecta Math. 29 (2023) art. id. 53 MR Zbl

[3] **H Geiges**, *A contact geometric proof of the Whitney–Graustein theorem*, Enseign. Math. 55 (2009) 93–102 MR Zbl

[4] **P Ghiggini**, *Knot Floer homology detects genus-one fibred knots*, Amer. J. Math. 130 (2008) 1151–1169 MR Zbl

[5] **J Hanselman**, **J Rasmussen**, **L Watson**, *Heegaard Floer homology for manifolds with torus boundary: properties and examples*, Proc. Lond. Math. Soc. 125 (2022) 879–967 MR Zbl

[6] **J Hanselman**, **J Rasmussen**, **L Watson**, *Bordered Floer homology for manifolds with torus boundary via immersed curves*, J. Amer. Math. Soc. 37 (2024) 391–498 MR Zbl

[7] **J Hanselman**, **L Watson**, *Cabling in terms of immersed curves*, Geom. Topol. 27 (2023) 925–952 MR Zbl

[8] **M Hedden**, *On knot Floer homology and cabling*, Algebr. Geom. Topol. 5 (2005) 1197–1222 MR Zbl

[9] **M Hedden**, **L Watson**, *On the geography and botany of knot Floer homology*, Selecta Math. 24 (2018) 997–1037 MR Zbl

[10] **J Hom**, *Bordered Heegaard Floer homology and the tau-invariant of cable knots*, J. Topol. 7 (2014) 287–326 MR Zbl

[11] **A Juhász**, **M Marengon**, *Concordance maps in knot Floer homology*, Geom. Topol. 20 (2016) 3623–3673 MR Zbl

[12] **Ç Karakurt**, **T Lidman**, *Rank inequalities for the Heegaard Floer homology of Seifert homology spheres*, Trans. Amer. Math. Soc. 367 (2015) 7291–7322 MR Zbl

[13] **A S Levine**, *Knot doubling operators and bordered Heegaard Floer homology*, J. Topol. 5 (2012) 651–712 MR Zbl

[14] **R Lipshitz**, **P S Ozsváth**, **D P Thurston**, *Bordered Heegaard Floer homology*, Mem. Amer. Math. Soc. 1216, Amer. Math. Soc., Providence, RI (2018) MR Zbl

[15] **Y Ni**, *Knot Floer homology detects fibred knots*, Invent. Math. 170 (2007) 577–608 MR Zbl

[16] **P Ozsváth**, **Z Szabó**, *Heegaard Floer homology and alternating knots*, Geom. Topol. 7 (2003) 225–254 MR Zbl

[17] **P Ozsváth**, **Z Szabó**, *Holomorphic disks and genus bounds*, Geom. Topol. 8 (2004) 311–334 MR Zbl

[18] **P Ozsváth**, **Z Szabó**, *Holomorphic disks and knot invariants*, Adv. Math. 186 (2004) 58–116 MR Zbl

[19] **I Petkova**, *Cables of thin knots and bordered Heegaard Floer homology*, Quantum Topol. 4 (2013) 377–409 MR Zbl

[20] **J A Rasmussen**, *Floer homology and knot complements*, PhD thesis, Harvard University (2003) MR arXiv math/0306378

[21] **H Whitney**, *On regular closed curves in the plane*, Compositio Math. 4 (1937) 276–284 MR Zbl

School of Mathematics, Georgia Institute of Technology
Atlanta, GA, United States

wshen41@gatech.edu

Received: 22 September 2022 Revised: 29 October 2023

ALGEBRAIC & GEOMETRIC TOPOLOGY

msp.org/agt

See inside back cover or msp.org/agt for submission instructions.

The subscription price for 2025 is US $760/year for the electronic version, and $1110/year (+$75, if shipping outside the US) for print and electronic. Subscriptions, requests for back issues and changes of subscriber address should be sent to MSP. Algebraic & Geometric Topology is indexed by Mathematical Reviews, Zentralblatt MATH, Current Mathematical Publications and the Science Citation Index.

Algebraic & Geometric Topology (ISSN 1472-2747 printed, 1472-2739 electronic) is published 9 times per year and continuously online, by Mathematical Sciences Publishers, c/o Department of Mathematics, University of California, 798 Evans Hall #3840, Berkeley, CA 94720-3840. Periodical rate postage paid at Oakland, CA 94615-9651, and additional mailing offices. POSTMASTER: send address changes to Mathematical Sciences Publishers, c/o Department of Mathematics, University of California, 798 Evans Hall #3840, Berkeley, CA 94720-3840.

AGT peer review and production are managed by EditFlow® from MSP.

PUBLISHED BY

mathematical sciences publishers

nonprofit scientific publishing

https://msp.org/

ALGEBRAIC & GEOMETRIC TOPOLOGY

Volume 25 Issue 6 (pages 3145–3787) 2025